Variability in snow cover phenology in China from 1952 to 2010

Chang-Qing Ke[1,2], Xiu-Cang Li[3,4], Hongjie Xie[5], Dong-Hui Ma[1, 6], Xun Liu[1,2] and Cheng Kou[1,2]

1. Jiangsu Provincial Key Laboratory of Geographic Information Science and Technology, Nanjing University, Nanjing, 210023, China.

2. Key Laboratory for Satellite Mapping Technology and Applications of State Administration of Surveying, Mapping and Geoinformation of China, Nanjing University, Nanjing, 210023, China.

3. National Climate Center, China Meteorological Administration, Beijing 100081, China.

4. Collaborative Innovation Center on Forecast and Evaluation of Meteorological Disasters， Faculty of Geography and Remote Sensing, Nanjing University of Information Science & Technology, Nanjing, 210044, China.

5. Department of Geological Sciences, University of Texas at San Antonio, Texas 78249, USA.

6. Collaborative Innovation Center of South China Sea Studies, Nanjing, 210023, China

Correspondence to: C. Q. Ke (kecq@nju.edu.cn)

Tel: 0086-25-89685860

Fax: 0086-25-83592686

Abstract Daily snow observation data from 672 stations, particularly the 296 stations with over ten annual mean snow cover days (SCD), during 1952–2010 in China, are used in this study. We first examine spatiotemporal variations and trends of SCD, snow cover onset date (SCOD), and snow cover end date (SCED). We then investigate SCD relationships with number of days with temperature below 0°C (TBZD), mean air temperature (MAT), and Arctic Oscillation (AO) index, the latter two being constrained to the snow season of each snow year. The results indicate that years with positive SCD anomaly for the entire country include 1955, 1957, 1964, and 2010, and years with negative SCD anomaly include 1953, 1965, 1999, 2002, and 2009. The reduced TBZD and increased MAT are the main reasons for the overall late SCOD and early SCED since 1952, although it is not necessary for one station to experience both significantly late SCOD and early SCED. This explains why only 12% of the stations show significant shortening of SCD, while 75% of the stations show no significant change in the SCD trends. This differs with the overall shortening of the snow period in the Northern Hemisphere previously reported. Our analyses indicate that the SCD distribution pattern and trends in China are very complex and are not controlled by any single climate variable examined (i.e. TBZD, MAT, or AO), but a combination of multiple variables. It is found that the AO has the maximum impact on the SCD shortening trends in the Shandong Peninsula, Changbai Mountains, Xiaoxingganling and North Xinjiang, while the combined TBZD and MAT have the maximum impact on the SCD shortening trends in the Loess Plateau, Tibetan Plateau, and Northeast Plain.

Keywords: snow cover day; snow cover onset date; snow cover end date; spatiotemporal variation; trend; days with temperature below 0°C; Arctic Oscillation

Abbreviations:

Snow Cover Day (SCD)

Snow Cover Onset Date (SCOD)

Snow Cover End Date (SCED)

Days with Temperature Below 0°C (TBZD)

Mean Air Temperature (MAT)

Arctic Oscillation (AO)

1 Introduction

Snow has a profound impact on the surficial and atmospheric thermal conditions, and is very sensitive to climatic and environmental changes, because of its high reflectivity, low thermal conductivity, and hydrological effects via snowmelt (Barnett et al., 1989; Groisman et al., 1994). The extent of snow cover in the Northern Hemisphere decreased significantly over the past decades because of global warming (Robinson and Dewey 1990; Brown and Robinson 2011). Snow cover showed the largest decrease in the spring, and the decrease rate increased for higher latitudes in response to larger albedo feedback (Déry and Brown, 2007). In North America, snow depth in central

Canada showed the greatest decrease (Dyer and Mote, 2006), and snowpack in the Rocky Mountains in the U.S. declined (Pederson et al., 2013). However, *in situ* data showed a significant increase in snow accumulation in winter but a shorter snowmelt season over Eurasia (Bulygina et al., 2009). Decrease in snow pack has also been found in the European Alps in the last 20 years of the 20th century (Scherrer et al., 2004), but a very long time series of snow pack suggests large decadal variability and overall weak long-term trends only (Scherrer et al., 2013). Meteorological data indicated that the snow cover over northwest China exhibited a weak upward trend in snow depth (Qin et al., 2006), with large spatiotemporal variations (Ke et al., 2009; Ma and Qin 2012). Simulation experiments using climate models indicated that, with continuing global warming, the snow cover in China would show more variations in space and time than ever before (Shi et al., 2011; Ji and Kang 2013). Spatiotemporal variations of snow cover are also manifested as snowstorms or blizzards, particularly excessive snowfall over a short time duration (Bolsenga and Norton, 1992; Liang et al., 2008; Gao, 2009; Wang et al., 2013; Llasat et al., 2014).

Snow cover day (SCD) is an important index that represents the environmental features of climate (Ye and Ellison 2003; Scherrer et al., 2004), and is directly related to the radiation and heat balance of the Earth–atmosphere system. The SCD varies in space and time and contributes to climate change over short time scales (Zhang, 2005), especially in the Northern Hemisphere. Bulygina et al. (2009) investigated the linear trends of SCD observed at 820 stations from 1966 to 2007, and indicated that the duration of snow cover decreased in the northern regions of European Russia and in the mountainous regions of southern Siberia, while it increased in Yakutia and the Far East. Peng et al. (2013) analysed trends in the snow cover onset date (SCOD) and snow cover end date (SCED) in relation to temperature over the past 27 years (1980–2006) from over 636 meteorological stations in the Northern Hemisphere. They found that the SCED remained stable over North America, whereas there was an early SCED over Eurasia. Satellite-derived snow data indicated that the average snow season duration over the Northern Hemisphere decreased at a rate of 5.3 days per decade between 1972/73 and 2007/08 (Choi et al., 2010). Their results also showed that a major change in the trend of snow duration occurred in the late 1980s, especially in the Western Europe, central and East Asia, and mountainous regions in western United States.

There are large spatiotemporal differences in the SCD in China (Wang and Li, 2012). Analysis of 40 meteorological stations from 1971 to 2010 indicated that the SCD had a significant decreasing trend in the western and south-eastern Tibetan Plateau, with the largest decline observed in Nielamu, reaching 9.2 days per decade (Tang et al., 2012). Data analysis also indicated that the SCD had a linear decreasing trend at most stations in the Hetao region and its vicinity (Xi et al., 2009). However, analysis of meteorological station data in Xinjiang showed that the SCD had a slight increasing trend, occurring mainly in 1960–1980 (Wang et al., 2009b). Li et al. (2009) analysed meteorological data from 80 stations in Heilongjiang Province, Northeast China. Their results showed that the snow cover duration shortened, because of both the late SCOD (by 1.9 days per decade) and early SCED (by 1.6 days per decade), which took place mainly in the lower altitude plains.

The SCD is sensitive to local winter temperature and precipitation, latitude (Hantel et al., 2000; Wang et al., 2009a; Serquet et al., 2011; Morán-Tejeda et al., 2013), and altitudinal gradient and terrain roughness (Lehning et al., 2011; Ke and Liu, 2014). Essentially, the SCD variation is mainly attributed to large-scale atmospheric circulation or climatic forcing (Beniston, 1997; Scherrer and Appenzeller, 2006; Ma and Qin, 2012; Birsan and Dumitrescu, 2014), such as monsoons, El Niño/Southern Oscillation (ENSO), North Atlantic Oscillation (NAO), and Arctic Oscillation (AO). Xu et al. (2010) investigated the relationship between the SCD and monsoon index in the Tibetan Plateau and indicated their great spatial differences. As an index of the dominant pattern of non-seasonal sea-level pressure variations, the AO shows a large impact on the winter weather patterns of the Northern Hemisphere (Thompson and Wallace, 1998; Thompson et al., 2000; Gong et al., 2001; Wu and Wang, 2002; Jeong and Ho, 2005). The inter-annual variation of winter extreme cold days in the northern part of eastern China is closely linked to the AO (Chen et al., 2013). Certainly, the AO plays an important role in the SCD variation. An increase in the SCD before 1990 and a decrease after 1990 have been reported in the Tibetan Plateau, and snow duration has positive correlations with the winter AO index (You et al., 2011), and a significant correlation between the AO and snowfall over the Tibetan Plateau on inter-decadal timescale was also reported by Lü et al. (2008).

The focus of this study is the variability in the snow cover phenology in China. A longer time series of daily observations of snow cover is used for these spatial and temporal analyses. We first characterize the spatial patterns of change in the SCD, SCOD, and SCED in different regions of China; we then examine the sensitivity of SCD to the number of days with temperature below 0°C (TBZD), the mean air temperature (MAT), and the Arctic Oscillation (AO) index during the snow season (between SCOD and SCED).

2 Data and methods

2.1 Data

We use daily snow cover and temperature data in China from the 1 September 1951 to the 31 August 2010, provided by the National Meteorological Information Centre of China Meteorological Administration (CMA). According to the Specifications for Surface Meteorological Observations (China Meteorological Administration, 2003), an SCD is defined as a day when the snow cover in the area meets the following requirement: at least half of the observation field is covered by snow. For any day with at least half of the observation field covered by snow, snow depth is recorded as a rounded-up integer. For example, a normal SCD is recorded if the snow depth is equal to or more than 1.0 cm (measured with a ruler), or a thin SCD if the snow depth is less than 1.0 cm. A snow year is defined at the time period from September 1 of the previous year to August 31 of the current year. For instance, September, October, and November 2009 are treated as the autumn season of snow year 2010, December 2009 and January and February 2010 as the winter season of snow year 2010, and March, April, and May 2010 as the spring season of snow year 2010.

Station density is high in eastern China, where the observational data for most stations are complete, with relatively long histories (as long as 59 years), while station density is low in western China, and the observation history is relatively short, although two of the three major snow regions are located in western China. If all stations with short time series are eliminated, the spatial representativeness of the dataset would be a problem. Therefore, a time series of at least 30 years is included in this study.

Because of topography and climate conditions, the discontinuous nature of snowfall is obvious in western China, especially in the Tibetan Plateau, with patchy snow cover, and there are many thin SCD records (Ke and Li, 1998). However, in order to enhance data reliability, thin SCDs in the original dataset are not taken into account in this paper according to the previous studies (An et al., 2009; Wang and Li, 2012).

Totally, there are 722 stations in the original dataset. Since station relocation and changes in the ambient environment could cause inconsistencies in the recorded data, we implement strict quality controls (such as inspection for logic, consistency, and uniformity) on the observational datasets in order to reduce errors (Ren et al., 2005). The standard normal homogeneity test (Alexandersson and Moberg, 1997) at the 95% confidence level is applied to the daily SCD and temperature series data in order to identify possible breakpoints. Time series gap filling is performed after all inhomogeneities are eliminated, using nearest neighbour interpolation. After being processed as mentioned above, the 672 stations with annual mean SCDs greater than 1.0 (day) are finally selected for subsequent investigation (Fig. 1).

The observation period for each station is different, varying between 59 years (1951/1952–2009/2010) and 30 years (1980/1981–2009/2010). Overall, 588 stations have observation records between 50 and 59 years, 47 stations between 40 and 49 years, and 37 stations between 30 and 39 years (Fig. 2). Most of the stations with observation records of less than 50 years are located in remote or high elevation areas. All 672 stations are used to analyse the spatiotemporal distribution of SCD in China, while only 296 stations with more than ten annual mean SCDs are used to study the changes of SCOD, SCED, and SCD relationships with TBZD, MAT, and the AO index.

The daily AO index constructed by projecting the daily (00Z) 1,000 mb height anomalies poleward of 20°N from http://www.cpc.ncep.noaa.gov/products/precip/CWlink/daily_ao_index/ao.shtml, is used. A positive (negative) AO index corresponds to low (high) pressure anomalies throughout the polar region and high (low) pressure anomalies across the subtropical and mid-latitudes (Peings et al., 2013). We average the daily AO indexes during the snow season of each station as the AO index of the snow year. A time series of AO indexes from 1952 to 2010, for each of the 296 stations, is then constructed.

A digital elevation model (DEM) from the Shuttle Radar Topographic Mission (SRTM, http://srtm.csi.cgiar.org) of the National Aeronautics and Space Administration (NASA) with a resolution of 90 m and the administration map of China are used as the base map.

2.2 Methods

We apply Mann–Kendall (MK) test to analyse the trends of SCD, SCOD, and SCED. The MK test is an effective tool to extract the trends of time series, and is widely applied to the analysis of climate series (Marty, 2008). The MK test is characterized as being more objective, since it is a non-parametric test. A positive standardized MK statistic value indicates an upward or increasing trend, while a negative value demonstrates a downward or decreasing trend. Confidence levels of 90% and 95% are taken as thresholds to classify the significance of positive and negative trends of SCD, SCOD, and SCED.

At the same time, if SCD, SCOD, or SCED at one climate station has significant MK trend (above 90%), their linear regression analyses are performed against time, respectively. The slopes of the regressions represent the changing trends and are expressed in days per decade. The statistical significance of the slope for each of the linear regressions is assessed by the Student's *t* test (two-tailed test of the Student *t* distribution), and only confidence levels above 90% are considered.

Correlation analysis is used to examine the SCD relationships with the TBZD, MAT, and the AO index, and the Pearson product-moment correlation coefficients (PPMCC) have been calculated. The PPMCC is a widely used estimator for describing the spatial dependence of rainfall processes, and it indicates the strength of the linear covariance between two variables (Habib et al., 2001; Ciach and Krajewski, 2006). The correlation coefficient can be defined as the covariance of the two variables (X, Y) divided by the product of their standard deviations, giving a value between +1 and −1 inclusive, where 1 is total positive correlation, 0 is no correlation, and −1 is total negative correlation. The statistical significance of the correlation coefficients is calculated using the Student's *t* test, and only confidence levels above 90% are considered in our analysis.

The spatial distribution of SCD, SCOD, and SCED, and their calculated results, are spatially interpolated by applying the universal kriging method (assuming the data is normally distributed). The universal kriging model is capable of simultaneously treating multiple variables and their cross-covariance, and has been successfully applied to spatial data interpolation (Kyriakidis and Goodchild, 2006). All mean errors are near zero, all average standard errors are close to the corresponding root mean squared errors, and all root mean squared standardized errors are close to 1 (Table 1). This fact indicates that prediction errors are unbiased and valid, except for slightly overestimated coefficients of variation (CV) and slightly underestimated SCD in 2002. Overall, the interpolation results have fewer errors and are acceptable.

3 Results

3.1 Spatiotemporal variations of SCD

3.1.1 Spatial distribution of SCD

The analysis of observations from 672 stations indicates that there are three major stable snow regions with more than 60 annual mean SCDs (Li, 1990): Northeast China, North Xinjiang, and the Tibetan Plateau, with Northeast China being the largest of the three (Fig. 3a). In the Daxingganling, Xiaoxingganling, and Changbai Mountains of Northeast China, there are more than 90 annual mean SCDs, corresponding to a relatively long snow season. The longest annual mean SCDs, 163 days, is at Arxan Station (in the Daxinganling Mountains) in Inner Mongolia. In North Xinjiang, the SCDs are relatively long in the Tianshan and Altun Mountains, followed by the Junggar Basin. The annual mean SCDs in the Himalayas, Nyainqentanglha, Tanggula Mountains, Bayan Har Mountains, Anemaqen Mountains, and Qilian Mountains of the

Tibetan Plateau are relatively long, although most of these regions have less than 60 annual SCDs. The Tibetan Plateau has a high elevation, a cold climate, and many glaciers, but its mean SCD is not as large as that of the other two stable snow regions.

Area with SCDs of 10–60 is called unstable snow regions with annual periodicity (definitely with snow cover in every winter) (Li, 1990). It includes the peripheral parts of the three major stable snow regions, Loess Plateau, Northeast Plain, North China Plain, Shandong Peninsula, and regions in north of the Qinling-Huaihe line (along the Qinling Mountains and Huaihe River to the east). Area with SCDs of 1–10 is called unstable snow region without annual periodicity (the mountainous regions are excluded) (Li, 1990). It includes the Qaidam Basin, Badain Jaran Desert, the peripheral parts of Sichuan Basin, the northeast part of the Yungui Plateau, and the middle and lower Yangtze River Plain. Areas with occasional snow and mean annual SCD of less than 1.0 (day) are distributed north of the Sichuan Basin and in the belt along Kunming, Nanling Mountains, and Fuzhou (approximate latitude of 25°N). Because of the latitude or local climate and terrain, there is no snow in the Taklimakan Desert, Turpan Basin, the Yangtze River Valley in the Sichuan Basin, the southern parts of Yunnan, Guangxi, Guangdong and Fujian, and on the Hainan Island.

The spatial distribution pattern of SCD based on climate data with longer time series is similar to previous studies (Li and Mi, 1983; Li, 1990; Liu et al., 2012; Wang et al., 2009a; Wang and Li, 2012). Snow distribution is closely linked to latitude and elevation, and is generally consistent with the climate zones (Lehning et al., 2011; Ke and Liu, 2014). There are relatively more SCDs in Northeast China and North Xinjiang, and fewer SCDs to the south (Fig. 3a). In the Tibetan Plateau, located in south-western China, the elevation is higher than eastern areas at the same latitude, and the SCDs are greater than in eastern China (Tang et al., 2012). The amount of precipitation also plays a critical role in determining the SCD (Hantel et al., 2000). In the north-eastern coastal areas of China, which are affected considerably by ocean, there is much precipitation. In North Xinjiang, which has a typical continental (inland) climate, the precipitation is less than in Northeast China, and there are more SCDs in the north of Northeast China than in North Xinjiang (Dong et al., 2004; Wang et al., 2009b). Moreover, the local topography has a relatively large impact on the SCD (Lehning et al., 2011). The Tarim Basin is located inland, with relatively little precipitation, thus snowfall there is extremely rare except in the surrounding mountains (Li, 1993). The Sichuan Basin is surrounded by high mountains, therefore situated in the precipitation shadow in winter, resulting in fewer SCDs (Li and Mi, 1983; Li, 1990).

The three major stable snow regions, Northeast China, North Xinjiang, and the eastern Tibetan Plateau, have smaller CV in the SCD (Fig. 3b). Nevertheless, the SCDs in arid or semi-arid regions, such as South Xinjiang, the northern and south-western Tibetan Plateau, and central and western Inner Mongolia, have large fluctuation because there is little precipitation during the cold seasons, and certainly little snowfall and large CVs of SCD. In particular, the Taklimakan Desert in the Tarim Basin is an extremely arid region, with only occasional snowfall. Therefore, it has a very large range of SCD fluctuations. Additionally, the middle and lower Yangtze River Plain also has large SCD fluctuations because of warm-temperate or sub-tropic climate with short winter and little snowfall. Generally, the smaller the SCD, the larger the CV (Wang et al., 2009a). This is consistent with other climate variables, such as precipitation (Yang et al., 2015).

3.1.2 Temporal variations of SCD

Seasonal variation of SCD is primarily controlled by temperature and precipitation (Hantel et al., 2000; Scherrer et al., 2004; Liu et al., 2012). In North Xinjiang and Northeast China, snow is primarily concentrated in the winter (Fig. 4). In these regions, the SCD exhibits a 'single-peak' distribution. In the Tibetan Plateau, however, the seasonal variation of SCD is slightly different, i.e. more snow in the spring and autumn combined than in the winter. The mean temperature and precipitation at Dangxiong station (30°29′ N, 91°06′E, 4200.0 m) in winter are -7.73^{o} C and 7.92 mm, respectively, and those at Qingshuihe station (33°48′ N, 97°08′E, 4415.4 m) are -15.8^{o} C and 16.3 mm, respectively. It is too cold and dry to produce enough snow in the Tibetan Plateau (Hu and Liang, 2014)

The temporal variation of SCD shows very large differences from one year to another. We define a year with a positive (negative) SCD anomaly in the following way: for a given year, if 70% of the stations have a positive (negative) anomaly and 30% of the stations have an SCD larger (smaller) than the mean +/− one standard deviation (1SD), it is regarded as a year with a positive (negative) SCD anomaly. The years with a positive SCD anomaly in China are 1955, 1957, 1964, and 2010 (Table 2). Moreover, the stations with SCDs larger than the mean + 2SD account for 25% and 26% of all stations in 1955 and 1957, respectively, and these two years are considered as years with an extremely positive SCD anomaly. In 1957, there was an almost nationwide positive SCD anomaly except for North Xinjiang (Fig. 5a). This 1957 event had a great impact on agriculture, natural ecology, and social-economic systems, and resulted in a tremendous disaster (Hao et al., 2002). The year 2010 was also a year with a positive SCD anomaly in China. At the same time, blizzards occurred in North America and Europe (including Spain) (Llasat et al., 2014). Globally, an unusual cold weather pattern caused by high pressure (the AO) brought cold, moist air from the north. Many parts of the Northern Hemisphere experienced heavy snowfall and record-low temperatures, leading to, among other things, a number of deaths, widespread transport disruption, and power failures (http://en.wikipedia.org/wiki/Winter_of_2009–10_in_Europe, http://en.wikipedia.org /wiki/February_9–10,_2010_North_American_blizzard). The blizzards across the Texas and Oklahoma panhandles in 1957 (Bolsenga and Norton, 1992; Changnon and Changnon, 2006) and the east coast in 2010 were also recorded as the biggest snowstorms of the United States from 1888 to the present (http://www.crh.noaa.gov/mkx/?n=biggestsnowstorms-us).

Years with a negative SCD anomaly include 1953, 1965, 1999, 2002, and 2009 (Table 2). If there is too little snowfall in a specific year, a drought is possible. Drought resulting from little snowfall in the cold season is a slow process and can sometimes cause disasters. For example, East China displayed an apparent negative SCD anomaly in 2002 (Fig. 5b), and had very little snowfall, leading to an extreme winter drought in Northeast China, where snowfall is the primary form of winter precipitation (Fang et al., 2014).

Because of different atmospheric circulation backgrounds, vapour sources, and topographic conditions in different regions of China, there are great differences in the SCD even in one year. For example, in 2008, there were more SCDs and longer snow duration in the Yangtze River Basin, North China, and the Tianshan Mountains in Xinjiang (Fig. 5c), especially in the Yangtze River Basin, where large snowfall was normally not observed. However, four episodes of severe and persistent snow, extreme low temperatures, and freezing weather occurred in 2008, leading to a large-scale catastrophe in this region where there were no mitigation measures for this type of a disaster (Gao, 2009). As reported by the Ministry of Civil Affairs of China, the 2008 snow disaster killed 107 people and caused losses of US$ 15.45 billion. Both the SCDs and scale of economic damage broke records from the past five decades (Wang et al., 2008). On the contrary, in the same year (2008), there was no snow disaster in North Xinjiang, the Tibetan Plateau, and Pan-Bohai Bay region. Moreover, Northeast China had an apparent negative SCD anomaly (Fig. 5c).

There are great differences in the temporal variations of SCD even in the three major stable snow regions. If we redefine a year with a positive (negative) SCD anomaly, using a much higher standard that 80% of stations should have a positive (negative) anomaly and 40% of stations should have an SCD larger (smaller) than the mean +/- 1SD. It is found that 1957, 1973, and 2010 are years with a positive SCD anomaly in Northeast China, while 1959, 1963, 1967, 1998, 2002, and 2008 are years with a negative SCD anomaly there (Table 3, Fig. 5a–c). Years with a positive SCD anomaly in North Xinjiang include 1960, 1977, 1980, 1988, 1994, and 2010, and years with a negative SCD anomaly include 1974, 1995, and 2008 (Table 3, Fig. 5c). North Xinjiang is one of the regions prone to catastrophe, where frequent heavy snowfall greatly affects the development of animal husbandry (Hao et al., 2002).

Years with a positive SCD anomaly in the Tibetan Plateau include 1983 and 1990, whereas years with a negative SCD anomaly include 1965, 1969, and 2010 (Table 3). The climate in the Tibetan Plateau is affected by the Indian monsoon from the south, westerlies from the west, and the East Asian monsoon from the east (Yao et al., 2012). Therefore, there is a regional difference in the SCD within the Tibetan Plateau, and even a difference in the spatiotemporal distribution of snow disasters (Wang et al., 2013). Our results differ from the conclusions drawn by Dong et al. (2001), as they only used data from 26 stations, covering only a short period (1967–1996).

3.1.3 SCD trends

Changing trends of annual SCDs are examined, as shown in Figure 6a, and summarized in Table 4. Among the 296 stations, there are 35 stations (12%) with a significant negative trend, and 37 stations (13%) with a significant positive trend (both at the 90% level), while 75% of stations show no significant trends. The SCD exhibits a significant downward trend in the Xiaoxingganling, the Changbai Mountains, the Shandong Peninsula, the Qilian Mountains, the North Tianshan Mountains, and the peripheral zones in the south and eastern Tibetan Plateau (Fig. 6a). For example, the SCD decreased by 50 days from 1955 to 2010 at the Kuandian station in Northeast China, 28 days from 1954 to 2010 at the Hongliuhe station in Xinjiang, and 10 days from 1958 to 2010 at the Gangcha station on the Tibetan Plateau (Fig. 7a–c).

The SCDs in the Bayan Har Mountains, the Anemaqen Mountains, the Inner Mongolia Plateau, and the Northeast Plain, exhibit a significant upward trend (Fig. 6a). For example, at the Shiqu station on the eastern border of the Tibetan Plateau, the SCD increased 26 days from 1960 to 2010 (Fig. 7d). The coexistence of negative and positive trends in the SCD change was also reported by Bulygina et al. (2009) and Wang and Li (2012).

3.2 Spatiotemporal variations of SCOD

3.2.1 SCOD variations

The SCOD is closely related to both latitude and elevation (Fig. 8a). For example, snowfall begins in September on the Tibetan Plateau, in early or middle October on the Daxingganling, and in middle or late October on the Altai Mountains in Xinjiang. The SCOD also varies from one year to another (Table 2). Using the definition of a year with a positive (negative) SCD anomaly, as introduced before (i.e. 70% stations with positive (negative) SCOD anomaly and 30% stations with SCOD larger (smaller) than the mean +/− 1SD), we consider a given year as a late (early) SCOD year. Two years, 1996 and 2006, can be considered as late SCOD years on a large scale (Table 2), especially in 2006, in East China and the Tibetan Plateau (Fig.5d). Only one year, 1982, can be considered as an early SCOD year.

3.2.2 SCOD trends

There are 196 stations (66%) with a significant trend of late SCOD, and 8 stations (3%) with a significant trend of early SCOD (both at the 90% level), while 31% of the stations show no significant trends (Table 4). The SCOD in the major snow regions in China exhibits a significant trend towards late SCOD (Fig. 6b). These significantly late trends dominate the major snow regions in China. In particular, the late SCOD in Northeast China is consistent with a previous study (Li et al., 2009). Only the SCOD in the East Liaoning Bay region exhibits a significant trend towards early SCOD. For example, the SCOD at the Pingliang station in Gansu Province shows a late rate of 5.2 days per decade from 1952 to 2010, but the SCOD at the Weichang station in Hebei Province shows an early rate of 5.2 days per decade from 1952 to 2010 (Fig. 7e–f).

3.3 Spatiotemporal variations of SCED

3.3.1 SCED variations

The pattern of SCED is similar to that of SCOD (Fig. 8b), i.e. places with early snowfall normally show late snowmelt, while places with late snowfall normally show early snowmelt. Like the SCOD, temporal variations of SCED are large (Table 2). Using the same standard for defining the SCOD anomaly, we judge a given year as a late (early) SCED year. Three years, 1957, 1976 and 1979, can be considered as late SCED years on a large scale (Table 2). It is evident that 1957 was a typical year whose SCED was late, which was also the reason for the great SCDs (Fig. 5a and e). The SCED in 1997 was early for almost all of China except for the Tibetan Plateau, western Tianshan Mountains, and western Liaoning (Fig. 5f).

3.3.2 SCED trends

For the SCED, there are 103 stations (35%) with a significantly early trend (at the 90% level), while 64% of stations show no significant trends (Table 4). The major snow regions in China all show early SCED, significant for Northeast China, North Xinjiang and the Tibetan Plateau (Fig. 6c). The tendency of late SCED is limited, with only 3 stations (1%) showing a significant trend. For example, the SCED at the Jixi station in Northeast China shows an early rate of 3.5 days per decade from 1952 to 2010, while the SCED at the Maerkang station in Sichuan Province shows a late rate of 4.2 days per decade from 1954 to 2010 (Fig. 7g–h).

4 Discussion

In the context of global warming, 196 stations (66%) show significantly late SCOD, and 103 stations (35%) show significantly early SCED, all at the 90% confidence level. It is not necessary for one station to show both significantly late SCOD and early SCED. This explains why only 12% of stations show a significantly negative SCD trend, while 75% of stations show no significant change in the SCD trends. The latter is inconsistent with the overall shortening of the snow period in the Northern Hemisphere reported by Choi et al. (2010). One reason could be the different time periods used in the two studies, 1972–2007 in Choi et al. (2010) as compared with 1952–2010 in this study. Below, we discuss the possible connections between the spatiotemporal variations of snow cover and the warming climate and changing AO.

4.1 Relationship with TBZD

The number of days with temperature below 0°C (TBZD) plays an important role in the SCD. There are 280 stations (95% of 296 stations) showing positive correlations between TBZD and SCD, with 154 of them (52%) having significantly positive correlations (Table 4, Fig. 6d). For example, there is a significantly positive correlation between SCD and TBZD at the Chengshantou station (Fig. 9a). Therefore, generally speaking, the smaller the TBZD, the shorter the SCD.

For the SCOD, there are 245 stations with negative correlations with TBZD, accounting for 83% of 296 stations, whereas only 51 stations (17%) show positive correlations (Table 4). This means that for smaller TBZD, the SCOD is later. For the SCED, there are 269 stations with positive correlations, accounting for 91% of 296 stations, whereas only 27 stations (9%) have negative correlations. This means that for smaller TBZD, the SCED is earlier.

Very similar results are found for the MAT (Table 4, Fig. 6e), and Fig. 9b shows an example (the Tieli station).

4.2 Relationship with AO

Although the AO index showed a strong positive trend in the past decades (Thompson et al., 2000), its impact on the SCD in China is spatially distinctive. Positive correlations (46% of 296 stations) are found in the eastern Tibetan Plateau and the Loess Plateau (Table 4, Fig. 6f), and Fig. 9c shows an example (the Huajialing station). Negative correlations (54% of 296 stations) exist in North Xinjiang, Northeast China and the Shandong Peninsula, and Fig. 9d shows an example (the Tonghua station).

5 Conclusion

This study examines the snow cover change based on 672 stations in 1952–2010 in China. Specifically, the 296 stations with more than ten annual mean SCDs are used to study the changing trends of SCD, SCOD, and SCED, and SCD relationships with

TBZD, MAT, and AO index during snow seasons. Some important results are summarized below.

Northeast China, North Xinjiang, and the Tibetan Plateau are the three major snow regions, with Northeast China being the largest. In North Xinjiang and in central and north-eastern China, the SCDs are concentrated in the winter season. On the Tibetan Plateau, however, snowfall is more frequent in the spring and fall. The overall inter-annual variability of SCD is large in China. The years with a positive SCD anomaly in China include 1955, 1957, 1964, and 2010, while the years with a negative SCD anomaly are 1953, 1965, 1999, 2002, and 2009. Only 12% of stations show a significantly negative SCD trend, while 75% of stations show no significant SCD trends. This differs from the overall shortening of the snow period in the Northern Hemisphere previously reported. One reason could be the different time periods used in the two studies, 1972–2007 in the work of Choi et al. (2010) compared with 1952–2010 in this study. Our analyses indicate that the SCD distribution pattern and trends in China are very complex and are not controlled by any single climate variable examined (i.e. TBZD, MAT, or AO), but a combination of multiple variables. However, it seems that the AO has the most impact on the SCD shortening trends in the Shandong Peninsula, Changbai Mountains, Xiaoxingganling, and North Xinjiang; the combination of smaller TBZD and increasing MAT has the largest impact on the SCD shortening trends on the Tibetan Plateau, the Loess Plateau, and the Northeast Plain.

It is found that significantly late SCOD occurs in nearly the entire China except for the east Liaoning Bay region; significantly early SCED occurs in nearly all major snow regions in China. Both the SCOD and SCED are closely related to the TBZD and MAT, and are mostly controlled by local latitude and elevation. Owing to global warming since 1950s, the reduced TBZD and increased MAT are the main reasons for overall late SCOD and early SCED, although it is not necessary for one station to experience both significantly late SCOD and early SCED. This explains why only 12% of stations show significantly negative SCD trends, while 75% of stations show no significant SCD trends.

Long-duration, consistent records of snow cover and depth are rare in China because of many challenges associated with taking accurate and representative measurements, especially in western China; the station density and metric choice also vary with time and locality. Therefore, more accurate and reliable observation data are needed to further analyse the spatiotemporal distribution and features of snow cover phenology. Atmospheric circulation causes variability in the snow cover phenology, and its effect requires deeper investigations.

Acknowledgments

This work is financially supported by the Program for National Nature Science Foundation of China (No. 41371391), and the Program for the Specialized Research Fund for the Doctoral Program of Higher Education of China (No. 20120091110017). This work is also partially supported by Collaborative Innovation Center of Novel Software Technology and Industrialization. We would like to thank the National Climate Center of China (NCC) in Beijing for providing valuable climate datasets. We thank the three anonymous reviewers and the editor for valuable comments and suggestions that greatly improved the quality of this paper.

References

An, D., Li, D., Yuan, Y. and Hui, Y.: Contrast between snow cover data of different definitions, J. Glaciol. Geocrol., 31(6), 1019-1027, 2009.

Alexandersson, H. and Moberg, A.: Homogenization of Swedish temperature data Part 1: homogeneity test for linear trends, Int. J. Climatol., 17, 25-34, 1997.

Barnett, T. P., Dumenil, L. and Latif, M.: The effect of Eurasian snow cover on regional and global climate variations, J. Atmos. Sci., 46, 661-685, 1989.

Beniston, M: Variations of snow depth and duration in the Swiss Alps over the last 50 years: Links to changes in large-scale climatic forcings, Clim. Change, 36, 281-300, 1997.

Birsan, M. V. and Dumitrescu, A.: Snow variability in Romania in connection to large-scale atmospheric circulation, Int. J. Climatol., 34, 134-144, 2014.

Bolsenga, S. J., and Norton, D. C.: Maximum snowfall at long-term stations in the U.S./Canadian Great Lakes, Nat. Hazards, 5, 221-232, 1992.

Brown, R. D. and Robinson, D. A.: Northern Hemisphere spring snow cover variability and change over 1922-2010 including an assessment of uncertainty, The Cryosphere, 5, 219-229, 2011.

Bulygina, O. N., Razuvaev, V. N. and Korshunova, N. N.: Changes in snow cover over Northern Eurasia in the last few decades, Environ. Res. Lett., 4, 045026, 2009.

Changnon, S. A. and Changnon, D.: A spatial and temporal analysis of damaging snowstorms in the United States, Nat. Hazards, 37, 373-389, 2006.

Chen, S., Chen, W. and Wei, K.: Recent trends in winter temperature extremes in eastern China and their relationship with the Arctic Oscillation and ENSO, Adv. Atmos. Sci., 30, 1712-1724, 2013.

China Meteorological Administration: Specifications for Surface Meteorological Observations, Beijing, China Meteorological Press, 1-62, 2003.

Choi, G., Robinson, D. A. and Kang, S.: Changing Northern Hemisphere snow seasons, J. Climate, 23, 5305-5310, 2010.

Ciach, G. J. and Krajewski, W. F.: Analysis and modeling of spatial correlation structure in small-scale rainfall in Central Oklahoma, Adv. Water Resour., 29(10), 1450–1463, 2006.

Déry, S. J. and Brown, R. D.: Recent Northern Hemisphere snow cover extent trends and implications for the snow-albedo feedback, Geophys. Res. Lett., 34, L22504, 2007.

Dong, A., Guo, H., Wang, L. and Liang, T.: A CEOF analysis on variation about yearly snow days in Northern Xinjiang in recent 40 years, Plateau Meteorol., 23, 936-940, 2004.

Dong, W., Wei, Z. and Fan, J.: Climatic character analysis of snow disasters in east Qinghai-Xizang Plateau livestock farm, Plateau Meteorol., 20, 402-406, 2001.

Dyer, J. L. and Mote, T. L.: Spatial variability and trends in observed snow depth over North America, Geophys. Res. Lett., 33, L16503, 2006

Fang, S., Qi, Y., Han, G., Zhou, G. and Cammarano, D.: Meteorological drought trend in winter and spring from 1961 to 2010 and its possible impacts on wheat in wheat planting area of China, Sci. Agricul. Sin., 47, 1754-1763, 2014

Gao, H.: China's snow disaster in 2008, who is the principal player? Int. J. Climatol., 29, 2191-2196, 2009.

Gong, D. Y., Wang, S. W. and Zhu, J. H.: East Asian winter monsoon and Arctic oscillation, Geophys. Res. Lett., 28, 2073-2076, 2001.

Groisman, P. Y., Karl, T. R. and Knight, R. W.: Observed impact of snow cover on the heat-balance and the rise of continental spring temperatures, Science, 263, 198-200, 1994.

Habib, E., Krajewski, W. F. and Ciach, G. J.: Estimation of rainfall interstation correlation, J. Hydrometeorol., 2(6), 621–629, 2001.

Hantel, M., Ehrendorfer, M. and Haslinger, A.: Climate sensitivity of snow cover duration in Austria, Int. J. Climatol., 20, 615-640, 2000.

Hao, L., Wang, J., Man, S. and Yang, C.: Spatio-temporal change of snow disaster and analysis of vulnerability of animal husbandry in China, J. Nat. Disaster, 11, 42-48, 2002.

He, L. and Li, D.: Classification of snow cover days and comparing with satellite remote sensing data in west China, J. Glaciol. Geocrol., 33(2), 237-245, 2011.

Hu, H. and Liang, L.: Temporal and spatial variations of snowfall in the east of Qinghai-Tibet Plateau in the last 50 years, Acta Geogr. Sin., 69, 1002-1012, 2014.

Jeong, J. H. and Ho, C. H.: Changes in occurrence of cold surges over East Asia in association with Arctic oscillation, Geophys. Res. Lett., 32, L14704, 2005.

Ji, Z. and Kang, S.: Projection of snow cover changes over China under RCP scenarios Clim. Dyn., 41, 589-600, 2013.

Ke, C. Q. and Li, P. J.: Spatial and temporal characteristics of snow cover over the Tibetan plateau, Acta Geogr. Sin., 53, 209-215, 1998.

Ke, C. Q. and Liu, X.: MODIS-observed spatial and temporal variation in snow cover in Xinjiang, China, Clim. Res., 59, 15-26, 2014.

Ke, C. Q., Yu, T., Yu, K., Tang, G. D. and King, L.: Snowfall trends and variability in Qinghai, China, Theor. Appl. Climatol., 98, 251-258, 2009.

Kyriakidis, P. C. and Goodchild, M. F.: On the prediction error variance of three common spatial interpolation schemes, Int. J. Geogr. Info. Science, 20(8), 823-855, 2006.

Lehning, M., Grünewald, T. and Schirmer, M.: Mountain snow distribution governed by an altitudinal gradient and terrain roughness, Geophys. Res. Lett., 38, L19504, 2011.

Li, D., Liu, Y., Yu, H. and Li, Y.: Spatial-temporal variation of the snow cover in Heilongjiang Province in 1951-2006, J. Glaciol. Geocrol., 31, 1011-1018, 2009.

Li, J. and Wang, J.: A modified zonal index and its physical sense, Geophys. Res. Lett., 30, 1632, 2003.

Li, L. Y. and Ke, C. Q.: Analysis of spatiotemporal snow cover variations in Northeast China based on moderate-resolution-imaging spectroradiometer data, J. Appl. Remote Sens., 8, 084695, doi: 10.1117/1.JRS.8.084695. 2014.

Li, P. J.: Dynamic characteristic of snow cover in western China, Acta Meteorol. Sin., 48, 505-515, 1993.

Li, P. J.: A preliminary study of snow mass variations over past 30 years in China, Acta Geogr. Sin., 48, 433-437, 1990.

Li, P. J. and Mi, D.: Distribution of snow cover in China, J. Glaciol. Geocrol., 5, 9-18, 1983.

Liang, T. G., Huang, X. D., Wu, C. X., Liu, X. Y., Li, W. L., Guo, Z. G. and Ren, J. Z.: An application of MODIS data to snow cover monitoring in a pastoral area: A case study in Northern Xinjiang, China, Remote Sens. Environ., 112, 1514-1526, 2008.

Liu, Y., Ren, G. and Yu, H.: Climatology of Snow in China, Sci. Geogr. Sin., 32, 1176-1185, 2012.

Llasat, M. C., Turco, M., Quintana-Seguí, P. and Llasat-Botija, M.: The snow storm of 8 March 2010 in Catalonia (Spain): a paradigmatic wet-snow event with a high societal impact, Nat. Hazards Earth Syst. Sci., 14, 427-441, 2014.

Lü, J. M., Ju, J. H., Kim, S. J., Ren, J. Z. and Zhu, Y. X.: Arctic Oscillation and the autumn/winter snow depth over the Tibetan Plateau, J. Geophys. Res., 113, D14117, 2008.

Ma, L. and Qin, D.: Temporal-spatial characteristics of observed key parameters of snow cover in China during 1957-2009, Sci. Cold Arid Reg., 4, 384-393, 2012.

Marty, C.: Regime shift of snow days in Switzerland, Geophys. Res. Lett., 35, L12501, 2008.

Morán-Tejeda, E., López-Moreno, J. I. and Beniston, M.: The changing roles of temperature and precipitation on snowpack variability in Switzerland as a function of altitude, Geophys. Res. Lett., 40, 2131-2136, 2013.

Pederson, G. T., Betancourt, J. L. and Gregory, J. M.: Regional patterns and proximal causes of the recent snowpack decline in the Rocky Mountains, U.S., Geophys. Res. Lett., 40, 1811-1816, 2013.

Peings, Y., Brun, B., Mauvais, V. and Douville, H.: How stationary is the relationship between Siberian snow and Arctic Oscillation over the 20th century, Geophys. Res. Lett., 40, 183-188, 2013.

Peng, S., Piao, S., Ciais, P., Fang, J. and Wang, X.: Change in winter snow depth and its impacts on vegetation in China, Glob. Change Biol., 16, 3004-3013, 2010.

Peng, S., Piao, S., Ciais, P., Friedlingstein, P., Zhou, L. and Wang, T.: Change in snow phenology and its potential feedback to temperature in the Northern Hemisphere over the last three decades, Environ. Res. Lett., 8, 014008, 2013.

Qin, D., Liu, S. and Li, P.: Snow cover distribution, variability, and response to climate change in western China, J. Climate, 19, 1820-1833, 2006.

Ren, G. Y., Guo, J., Xu, M. Z., Chu, Z. Y., Zhang, L., Zou, X. K., Li, Q. X. and Liu, X. N.: Climate changes of China's mainland over the past half century, Acta. Meteorol. Sin., 63, 942-956, 2005.

Robinson, D. A. and Dewey, K. F.: Recent secular variations in the extent of northern hemisphere snow cover, Geophys. Res. Lett., 17, 1557-1560, 1990.

Scherrer, S. C., Appenzeller, C. and Laternser, M.: Trends in Swiss Alpine snow days: The role of local- and large-scale climate variability, Geophys. Res. Lett., 31, L13215, 2004.

Scherrer, S. C. and Appenzeller, C.: Swiss Alpine snow pack variability: major patterns and links to local climate and large-scale flow, Clim. Res., 32(3), 187-199, 2006.

Scherrer, S. C., Wüthrich, C., Croci-Maspoli, M., Weingartner, R. and Appenzeller, C.: Snow variability in the Swiss Alps 1864-2009, Int. J. Clim., 33(15), 3162–3173, 2013, doi: 10.1002/joc.3653.

Serquet, G., Marty, C., Dulex, J-P. and Rebetez, M.: Seasonal trends and temperature dependence of the snowfall/precipitation-day ratio in Switzerland, Geophys. Res. Lett., 38, L07703, 2011.

Shi, Y., Gao, X., Wu, J. and Giorgi, F.: Changes in snow cover over China in the 21st century as simulated by a high resolution regional climate model, Environ. Res. Lett., 6, 045401, 2011.

Tang, X., Yan, X., Ni, M. and Lu, Y.: Changes of the snow cover days on Tibet Plateau in last 40 years, Acta. Geogr. Sin., 67, 951-959, 2012.

Thompson, D. W. J. and Wallace, J. M.: The Arctic oscillation signature in the wintertime geopotential height and temperature fields, Geophys. Res. Lett., 25, 1297-1300, 1998.

Thompson, D. W. J., Wallace, J. M. and Hegerl, G. C.: Annular modes in the extratropical circulation, part II: Trends, J. Climate, 13, 1018-1036, 2000.

Wang, C. and Li, D.: Spatial-temporal variations of the snow cover days and the maximum depth of snow cover in China during recent 50 years, J. Glaciol. Geocrol., 34, 247-256, 2012.

Wang, C., Wang, Z. and Cui, Y.: Snow cover of China during the last 40 years: Spatial distribution and interannual variation, J. Glaciol. Geocrol., 31, 301-310, 2009a.

Wang, J. and Hao, X.: Responses of snowmelt runoff to climatic change in an inland river basin, Northwestern China, over the past 50 years, Hydrol. Earth Syst. Sci., 14, 1979-1987, 2010.

Wang, L. et al.: Characteristics of the extreme low-temperature, heavy snowstorm and freezing disasters in January 2008 in China, Meteorol. Mon., 34, 95-100, 2008.

Wang, Q., Zhang, C., Liu, J. and Liu, W.: The changing tendency on the depth and days of snow cover in Northern Xinjiang, Adv. Clim. Change Res., 5, 39-43, 2009b.

Wang, W., Liang, T., Huang, X., Feng, Q., Xie, H., Liu, X., Chen, M. and Wang, X.: Early warning of snow-caused disasters in pastoral areas on the Tibetan Plateau, Nat. Hazards Earth Syst. Sci., 13, 1411-1425, 2013.

Wu, B. Y. and Wang, J.: Winter Arctic oscillation, Siberian high and East Asian winter monsoon, Geophys. Res. Lett., 29, 1897, 2002.

Xi, Y., Li, D. and Wang, W.: Study of the temporal-spatial characteristics of snow covers days in Hetao and its vicinity, J. Glaciol. Geocrol., 31, 446-456, 2009.

Xu, L., Li, D. and Hu, Z.: Relationship between the snow cover day and monsoon index in Tibetan Plateau, Plateau Meterol., 29, 1093-1101, 2010.

Yang, H., Yang, D., Hu, Q. and Lv, H.: Spatial variability of the trends in climatic variables across China during 1961-2010, Theor. Appl. Climatol., 2015 (in press).

Yao, T. et al.: Different glacier status with atmospheric circulations in Tibetan Plateau and surroundings, Nature Clim. Change, 2, 663-667, 2012.

Ye, H. and Ellison, M.: Changes in transitional snowfall season length in northern Eurasia, Geophys. Res. Lett., 30, 1252, 2003.

You, Q., Kang, S., Ren, G., Fraedrich, K., Pepin, N., Yan, Y. and Ma, L.: Observed changes in snow depth and number of snow days in the eastern and central Tibetan Plateau, Clim. Res., 46, 171-183, 2011.

Zhang, T.: Influence of the seasonal snow cover on the ground thermal regime: An overview, Rev. Geophys., 43, 1-23, 2005.

Table Captions

Table 1. Prediction errors of cross validation for the spatial interpolation with the universal kriging method.

Item (Figures)	Mean error	Average standard error	Root mean squared error	Root mean squared standardized error
SCD (Fig.3a)	-0.0230	11.0558	13.7311	1.1097
CV (Fig.3b)	0.0017	0.7364	0.5510	0.7579
SCD in 1957 (Fig.5a)	-0.0015	11.1561	13.4662	1.1898
SCD in 2002 (Fig.5b)	0.0306	6.6185	8.5887	1.2522
SCD in 2008 (Fig.5c)	0.0477	7.3167	8.1968	1.0969
SCED in 1957 (Fig.5d)	-0.0449	15.0528	18.9860	1.1921
SCED in 1997 (Fig.5e)	0.0696	15.5722	17.7793	1.1040
SCOD in 2006 (Fig.5f)	0.0482	15.4503	16.1757	1.0449
SCOD (Fig.8a)	0.0293	11.2458	13.9078	1.1712
SCED (Fig.8b)	-0.0222	15.2265	18.3095	1.1308

Table 2. Percentage (%) of stations with anomalies (P for positive and N for negative) of snow cover day (SCD), snow cover onset date (SCOD), and snow cover end date (SCED). Percentage (%) of stations with anomalies of SCD, SCOD, and SCED larger (smaller) than the mean +/- one or two standard deviations (1SD or 2SD), with the bold number denoting years with a positive (negative) SCD anomaly, and late (early) years for SCOD or SCED in China. All the percentages are calculated based on 672 stations.

	SCD					SCOD						SCED					
Year	P	1SD	2SD	-2SD	-1SD	N	P	1SD	2SD	-2SD	-1SD	N	P	1SD	2SD	-2SD	-1SD	N
1952	31	2	0	13	33	69	69	40	21	2	9	31	55	17	2	12	17	45
1953	28	7	0	**3**	**36**	**72**	40	8	2	2	18	60	37	8	1	10	18	63
1954	57	31	12	0	8	43	35	8	4	1	18	65	56	11	0	0	10	44
1955	**79**	**45**	**25**	1	5	21	37	9	4	1	22	63	77	21	2	1	6	23
1956	46	10	0	0	4	54	69	20	2	0	9	31	61	24	1	2	12	39
1957	**85**	**62**	**26**	0	3	15	26	6	1	0	15	74	**84**	**35**	**5**	1	4	16
1958	48	15	4	0	14	52	46	17	0	0	18	54	52	17	3	4	18	48
1959	28	7	1	4	23	72	53	26	8	1	18	47	59	23	3	1	5	41
1960	37	13	3	0	16	63	49	11	2	0	10	51	59	24	6	4	18	41
1961	36	7	1	1	18	64	25	9	2	1	27	75	30	6	1	7	26	70
1962	41	11	3	0	10	59	44	13	4	2	10	56	58	18	3	0	11	42
1963	25	5	2	2	27	75	34	14	5	1	23	66	51	14	0	8	17	49
1964	**76**	**36**	**11**	0	1	24	31	3	1	4	24	69	64	18	1	0	5	36
1965	26	8	0	**1**	**32**	**74**	59	18	5	1	8	41	55	14	2	3	17	45
1966	28	6	1	0	13	72	46	21	6	0	13	54	67	12	1	2	5	33
1967	31	5	0	3	23	69	40	11	3	2	15	60	43	5	0	3	12	57
1968	61	29	12	3	8	39	35	8	1	0	13	65	34	13	0	4	26	66
1969	42	18	5	4	21	58	45	13	1	3	20	55	67	20	1	1	7	33
1970	46	15	1	2	11	54	38	10	3	2	24	62	62	19	3	0	7	38
1971	53	12	1	1	9	47	38	15	4	1	17	62	53	9	1	1	8	47
1972	55	23	11	0	8	45	37	9	2	1	21	63	46	16	4	1	9	54
1973	50	19	2	1	7	50	35	10	1	2	23	65	43	9	1	1	8	57
1974	33	8	0	3	23	67	53	29	6	1	11	47	52	12	1	1	10	48
1975	41	10	4	1	15	59	26	7	2	1	21	74	43	15	3	2	16	57
1976	35	11	3	1	23	65	60	25	12	0	5	40	**77**	**31**	**5**	1	3	23
1977	45	20	3	0	9	55	28	5	1	0	25	72	57	14	3	2	12	43
1978	60	22	8	0	2	40	43	13	2	2	13	57	55	10	1	0	8	45
1979	41	8	1	0	7	59	43	11	1	0	20	57	**79**	**32**	**2**	0	4	21
1980	39	12	1	0	5	61	41	9	1	1	16	59	82	27	2	0	4	18

1981	42	13	2	0	13	58	45	20	4	2	18	55	44	13	1	2	15	56
1982	40	12	1	1	15	60	23	9	2	**0**	**30**	**77**	58	23	6	6	16	42
1983	50	19	6	0	12	50	44	14	1	1	11	56	67	26	2	1	9	33
1984	26	9	1	1	28	74	68	32	16	0	5	32	48	8	1	2	13	52
1985	66	24	3	0	3	34	32	8	1	1	24	68	46	8	2	1	8	54
1986	50	14	2	0	12	50	32	5	1	1	19	68	63	18	4	3	10	38
1987	67	23	4	0	4	33	40	7	1	2	15	60	60	23	3	1	8	40
1988	56	17	1	0	2	44	24	6	1	3	26	76	69	23	0	1	7	31
1989	47	18	4	0	11	53	71	29	7	1	6	29	41	6	1	3	18	59
1990	56	19	2	0	7	44	52	9	1	0	9	48	49	12	1	2	10	51
1991	34	4	0	2	9	66	60	21	3	0	4	40	72	26	3	1	4	28
1992	50	13	4	1	7	50	54	18	5	0	4	46	50	13	1	5	19	50
1993	58	19	2	1	4	42	43	9	1	0	17	57	49	18	2	2	21	51
1994	58	19	2	0	4	42	28	6	2	1	22	72	39	11	0	3	18	61
1995	36	10	3	3	15	64	57	24	3	1	15	43	49	8	1	7	18	51
1996	26	8	2	2	22	74	**71**	**30**	**4**	0	5	29	55	11	1	2	15	45
1997	37	3	0	1	18	63	44	13	3	2	12	56	18	4	2	**9**	**49**	**82**
1998	34	8	2	4	18	66	37	11	3	1	20	63	30	9	1	7	25	70
1999	25	4	1	**1**	**35**	**75**	61	23	12	1	7	39	51	11	2	5	15	49
2000	64	17	4	0	5	36	59	18	2	0	9	41	39	7	0	5	22	61
2001	67	29	8	0	5	33	39	16	2	1	22	61	42	17	1	3	15	58
2002	17	2	0	**5**	**32**	**83**	59	22	4	1	4	41	31	6	0	12	30	69
2003	57	29	4	1	8	43	36	6	1	0	21	64	50	9	2	6	18	50
2004	35	3	1	0	16	65	42	11	2	1	26	58	32	7	1	13	33	68
2005	60	18	1	0	4	40	48	15	2	0	11	52	33	4	0	2	19	67
2006	48	11	3	0	8	52	**70**	**33**	**7**	0	5	30	57	16	0	1	10	43
2007	30	6	1	0	22	70	69	25	5	1	6	31	29	3	1	7	26	71
2008	43	19	5	3	20	57	68	27	7	0	8	32	41	10	1	4	24	59
2009	24	6	0	**1**	**31**	**76**	73	23	9	0	5	27	27	4	0	3	25	73
2010	**75**	**42**	**11**	0	10	25	42	11	2	1	18	58	72	20	1	1	7	28

Table 3. The same as Table 2, but only for the years with a positive (negative) SCD anomaly and only for the three major stable snow regions: Northeast China (78 stations), North Xinjiang (21 stations) and the Tibetan Plateau (63 stations).

	Northeast China						North Xinjiang						Tibetan Plateau					
Year	P	1SD	2SD	-2SD	-1SD	N	P	1SD	2SD	-2SD	-1SD	N	P	1SD	2SD	-2SD	-1SD	N
1957	**98**	**72**	**16**	0	0	2	22	0	0	2	33	78	74	52	13	0	4	26
1959	2	0	0	**15**	**73**	**98**	88	38	0	0	0	12	37	11	3	0	6	63
1960	39	14	1	0	26	61	**100**	**88**	**29**	0	0	0	23	0	0	3	30	77
1963	11	0	0	**6**	**41**	**89**	26	0	0	5	26	74	20	0	0	0	28	80
1965	66	24	0	1	16	34	21	0	0	0	37	79	12	4	0	**4**	**50**	**88**
1967	16	0	0	**14**	**59**	**84**	78	22	0	0	6	22	23	6	0	0	15	77
1969	21	1	0	15	43	79	78	28	0	0	6	22	4	0	0	**6**	**53**	**96**
1973	**89**	**60**	**4**	0	0	11	42	0	0	5	11	58	36	11	2	0	21	64
1974	55	18	0	3	21	45	5	0	0	**21**	**58**	**95**	38	3	0	2	14	62
1977	73	32	4	0	5	27	**95**	**74**	**0**	0	5	5	36	19	7	0	7	64
1980	65	18	1	0	8	35	**95**	**63**	**5**	0	0	5	45	10	2	0	3	55
1983	62	23	3	0	3	38	26	0	0	0	21	74	**95**	**60**	**19**	0	0	5
1988	70	23	0	0	3	30	**100**	**68**	**11**	0	0	0	52	22	5	0	2	48
1990	40	0	0	0	11	60	32	5	0	0	21	68	**81**	**41**	**3**	0	0	19
1994	94	29	1	0	0	6	**95**	**53**	**0**	0	0	5	46	14	2	0	11	54
1995	33	1	0	3	15	67	5	0	0	**21**	**74**	**95**	75	42	11	0	0	25
1998	4	0	0	**14**	**64**	**96**	63	5	0	5	11	37	82	39	12	0	0	18
2002	4	0	0	**19**	**63**	**96**	26	0	0	5	21	74	22	2	0	0	15	78
2008	7	0	0	**11**	**48**	**93**	5	0	0	**5**	**47**	**95**	59	6	0	2	14	41
2010	**92**	**69**	**17**	0	3	8	**100**	**67**	**11**	0	0	0	15	6	0	**2**	**50**	**85**

Table 4. Number of stations with SCD, SCOD, and SCED trends, number of stations with relationships of SCD, SCOD, and SCED, respectively, with TBZD, number of stations with relationship between SCD and MAT, and number of stations with relationship between SCD and AO (296 stations in total). All of them have two significance levels, the 90% and 95%.

		SCD			SCOD			SCED		
		95%	90%	I*	95%	90%	I*	95%	90%	I*
Trend	Positive	19	37	125	178	196	74	1	3	37
	Negative	26	35	99	5	8	18	72	103	153
TBZD	Positive	124	154	126	0	1	50	72	99	170
	Negative	1	1	15	61	87	158	0	2	25
MAT	Positive	0	2	22						
	Negative	114	148	124						
AO	Positive	31	45	90						
	Negative	33	48	113						

(Note: I* for insignificant trends or relations)

Figure Captions

Figure 1. Locations of weather stations and major basins, mountains and plains mentioned in the paper, overlying the digital elevation model for China.

Figure 2. Percentage of weather stations with different measurement lengths.

Figure 3. Annual mean snow cover days (SCDs) from 1980/81 to 2009/10 (a), and their coefficients of variation (CV) (b).

Figure 4. Seasonal variation of SCDs; the number in the centre denotes annual mean SCDs, the blue colour in the circle the SCDs for winter season, the green colour for spring, and the red colour for autumn.

Figure 5. SCD anomalies in 1957 (a), 2002 (b) and 2008 (c), anomaly of snow cover onset date (SCOD) in 2006 (d), and anomalies of snow cover end date (SCED) in 1957 (e) and 1997 (f).

Figure 6. Trends of annual mean SCDs (a), SCOD (b), and SCED (c) from the 296 stations of more than ten annual mean SCDs with Mann–Kendall test, and relationships among the SCD and day with temperature below 0°C (TBZD) (d), mean air temperature (MAT) (e), and Arctic Oscillation (AO) index (f).

Figure 7. SCD variations at Kuandian (40°43′ N, 124°47′E, 260.1 m) (a), Hongliuhe (41°32′ N, 94°40′E, 1573.8 m) (b), Gangcha (37°20′ N, 100°08′E, 3301.5 m) (c) and Shiqu (32°59′ N, 98°06′E, 4533.0 m) (d), SCOD at Pingliang (35°33′ N, 106°40′E, 1412.0 m) (e) and Weichang (41°56′ N, 117°45′E, 842.8 m) (f), and SCED at Jixi (45°18′ N, 130°56′E, 280.8 m) (g) and Maerkang (31°54′ N, 102°54′E, 2664.4 m) (h).

(The unit on the Y-axis in the figures e, f, g, h denotes the Julian day using 1st September as reference).

Figure 8. Spatial distribution of SCOD (a) and SCED (b) based on the stations with an average of more than ten SCDs.

Figure 9. SCD relationships with TBZD at Chengshantou (37°24′ N, 122°41′E, 47.7 m) (a), MAT at Tieli (46°59′ N, 128°01′E, 210.5 m) (b), and AO index at Huajialing (35°23′ N, 105°00′E, 2450.6 m) (c) and Tonghua (41°41′ N, 125°54′E, 402.9 m) (d).

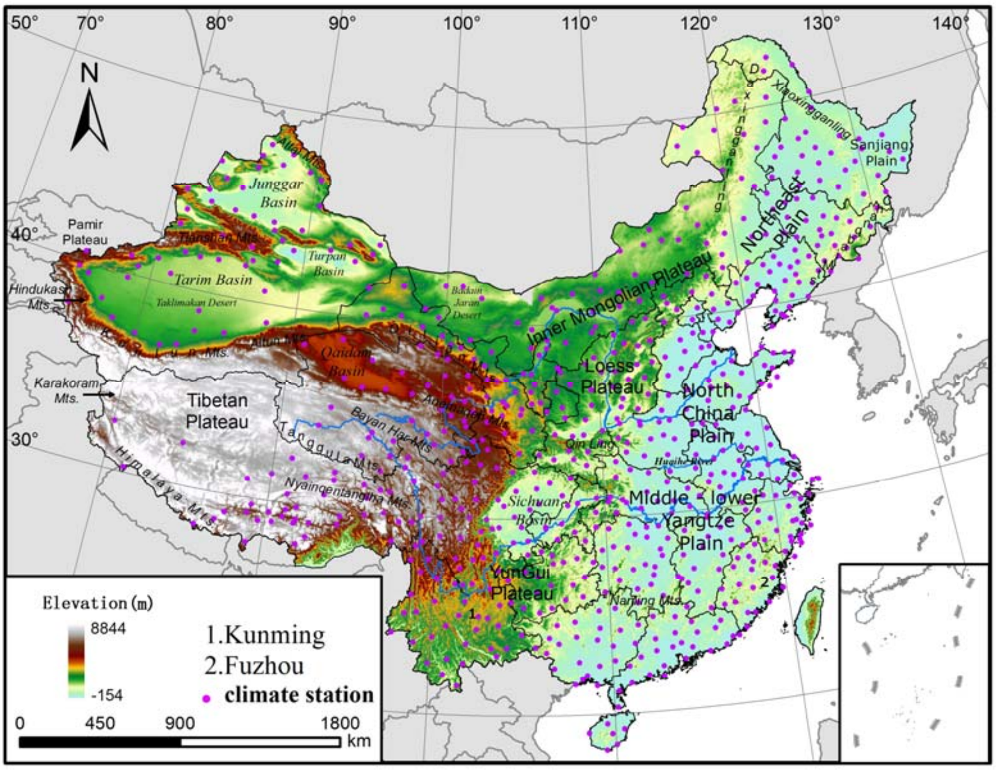

Figure 1

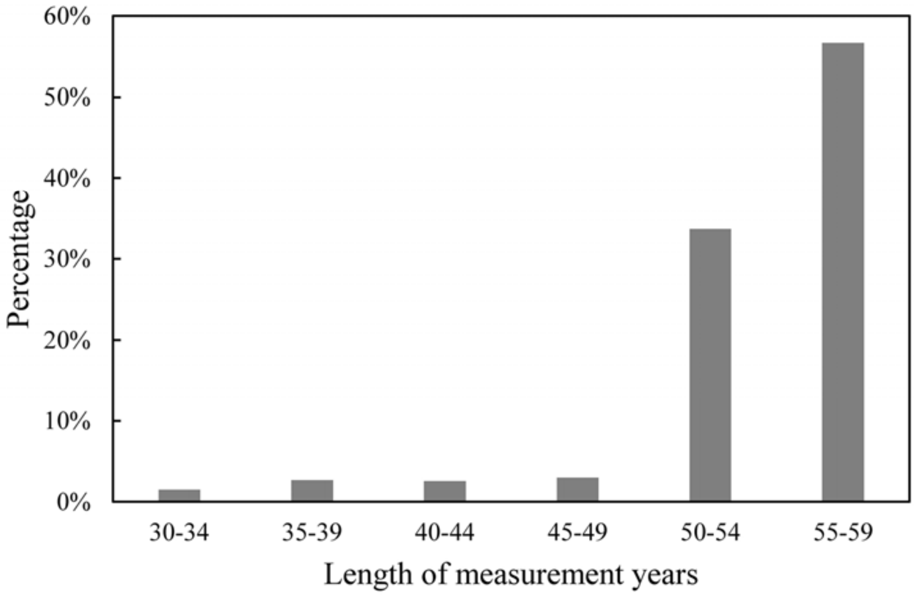

Figure 2

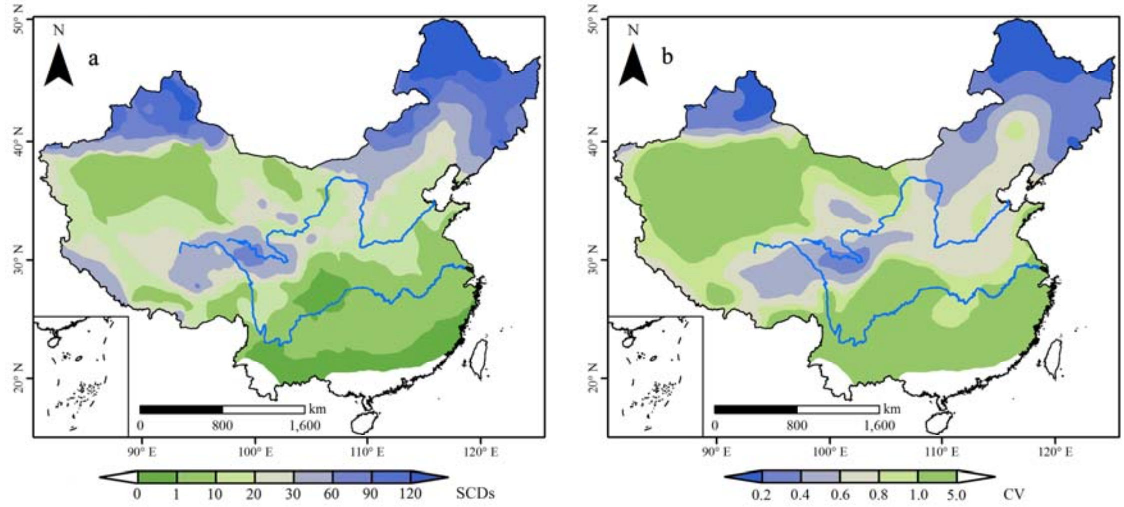

Figure 3

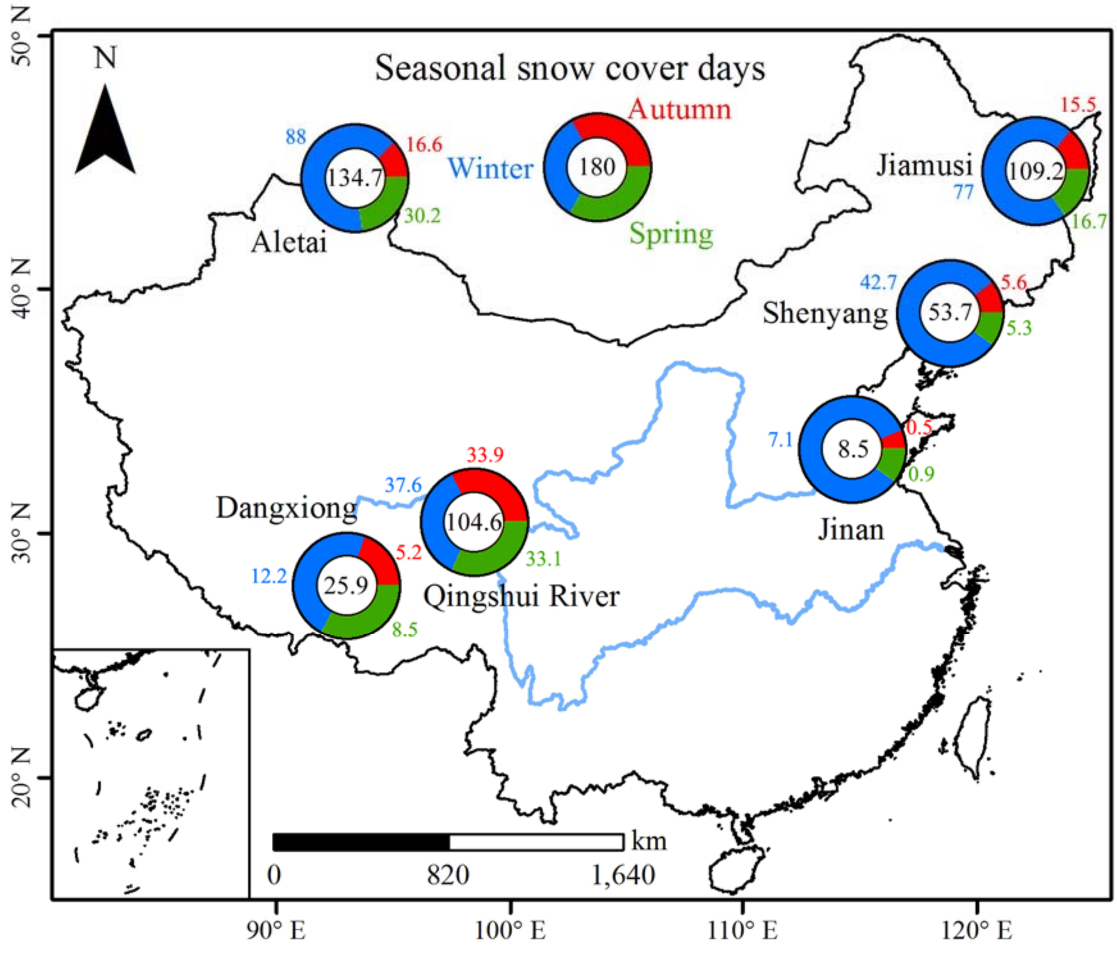

Figure 4

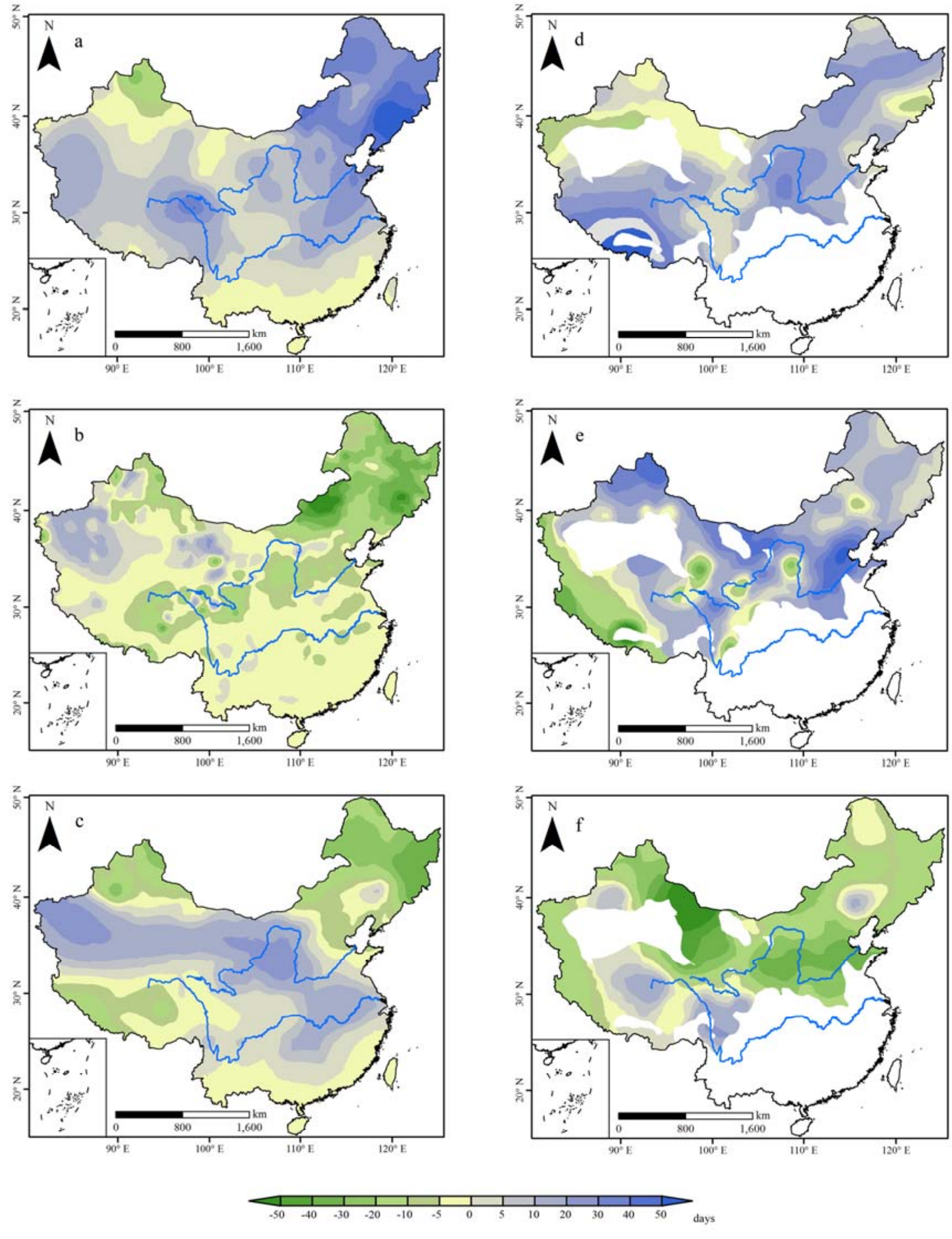
a
b
c
d
e
f
N
50° N
40° N
30° N
20° N
90° E
100° E
110° E
120° E
0
800
1,600
km
-50
-40
-30
-20
-10
-5
0
5
10
20
30
40
50
days

Figure 5

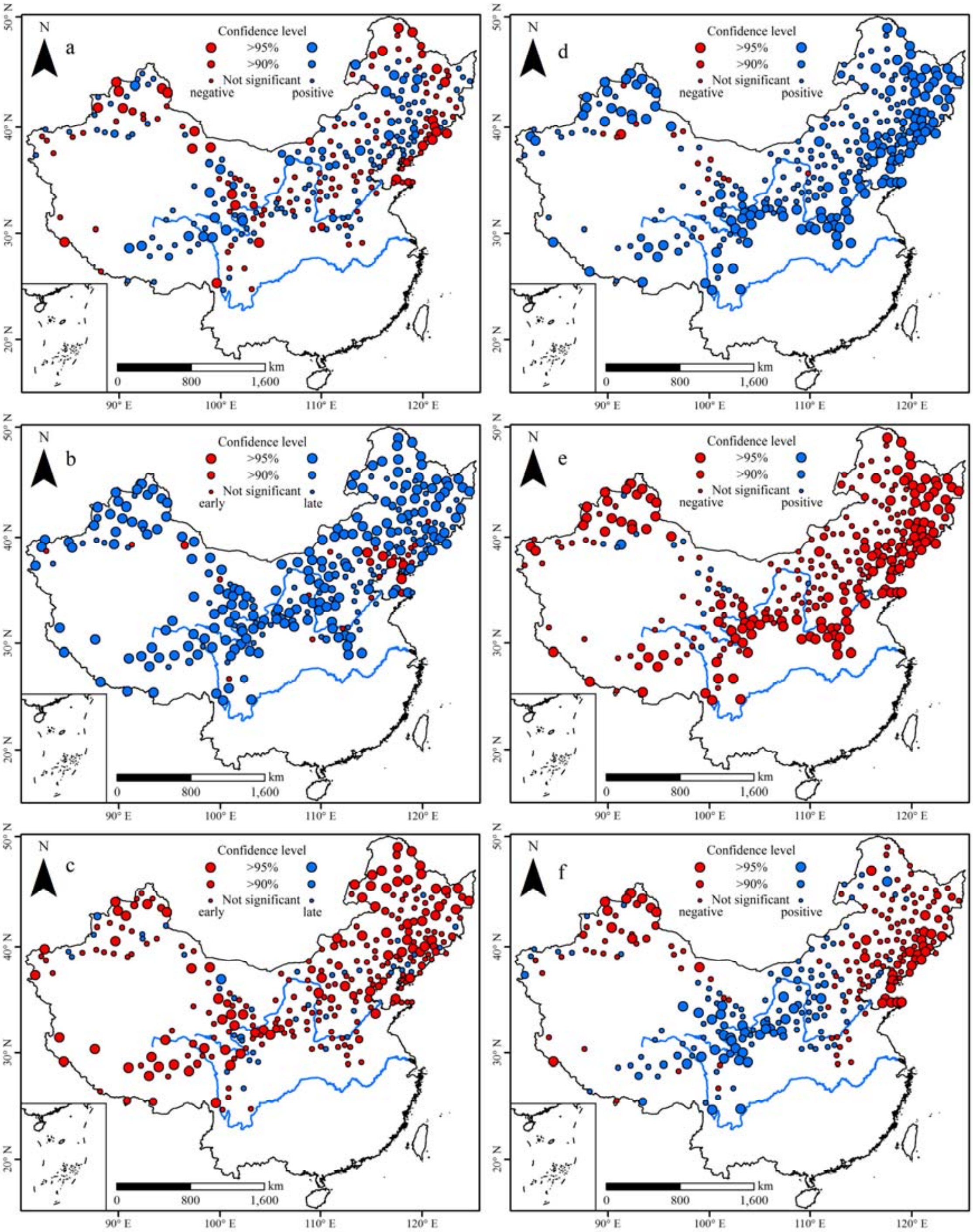

N
a
Confidence level
>95%
>90%
Not significant
negative
positive
b
early
late
c
d
e
f
km
0
800
1,600
50° N
40° N
30° N
20° N
90° E
100° E
110° E
120° E

Figure 6

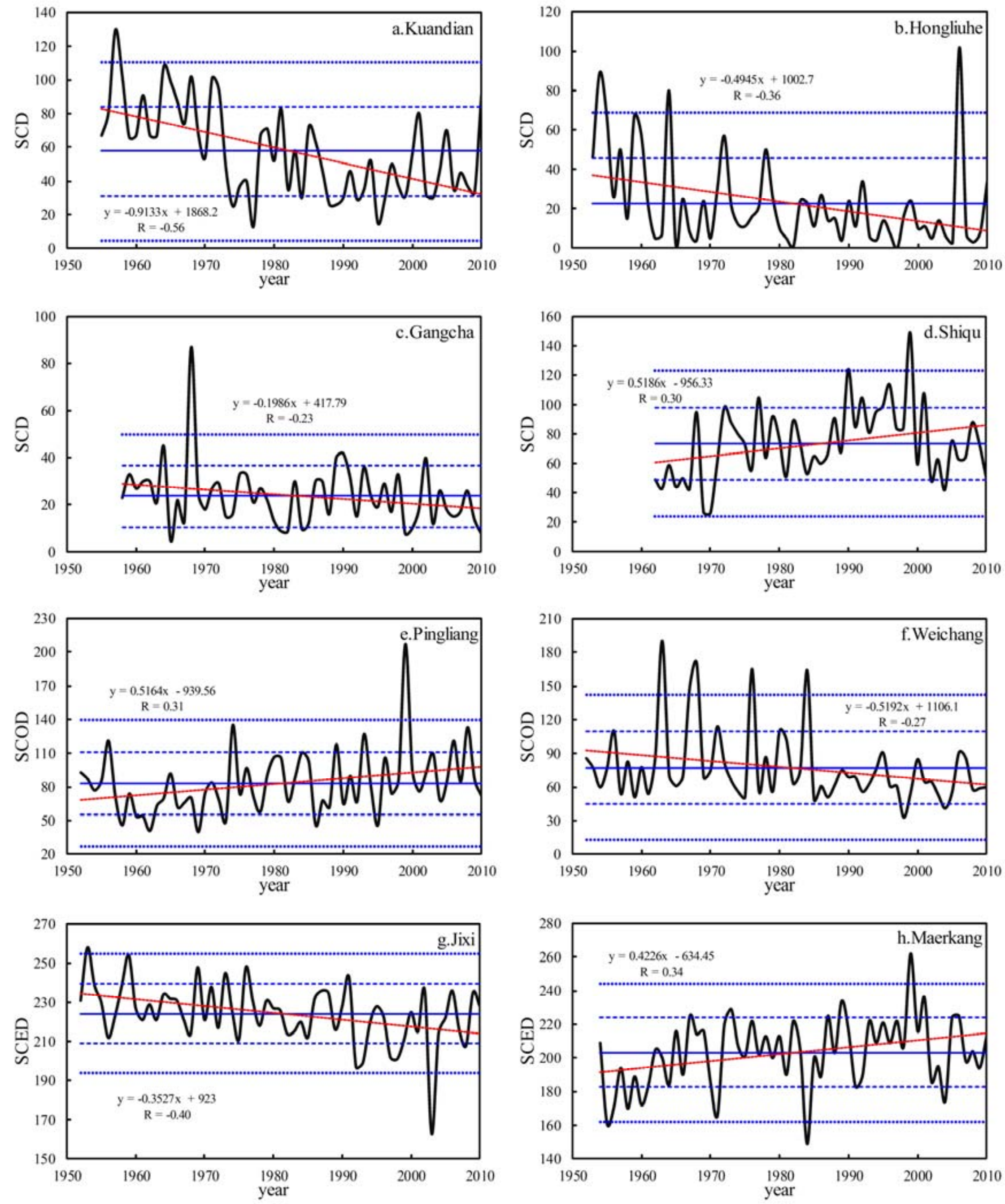
a.Kuandian
y = -0.9133x + 1868.2
R = -0.56
b.Hongliuhe
y = -0.4945x + 1002.7
R = -0.36
c.Gangcha
y = -0.1986x + 417.79
R = -0.23
d.Shiqu
y = 0.5186x - 956.33
R = 0.30
e.Pingliang
y = 0.5164x - 939.56
R = 0.31
f.Weichang
y = -0.5192x + 1106.1
R = -0.27
g.Jixi
y = -0.3527x + 923
R = -0.40
h.Maerkang
y = 0.4226x - 634.45
R = 0.34
SCD
SCOD
SCED
year

Figure 7

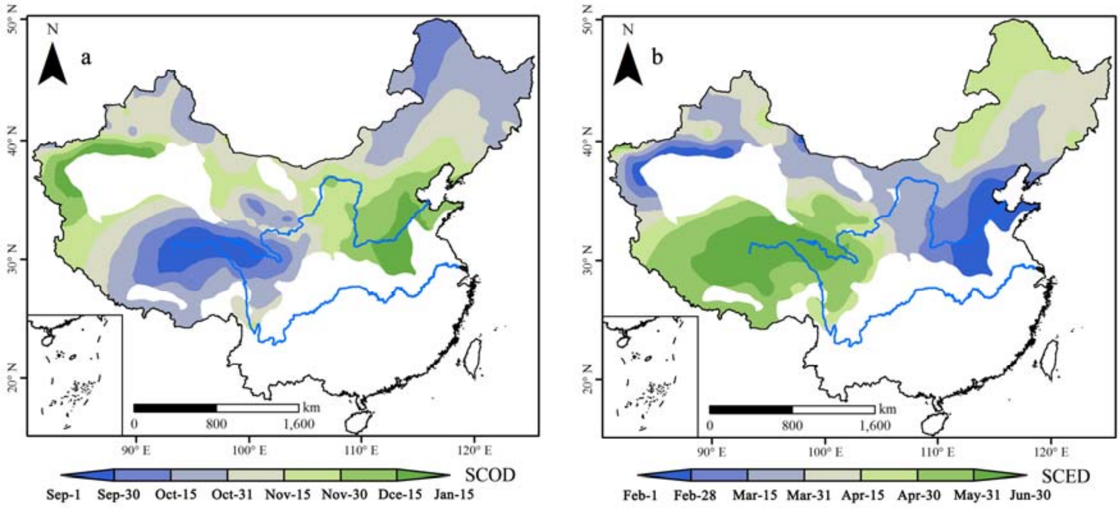

Figure 8

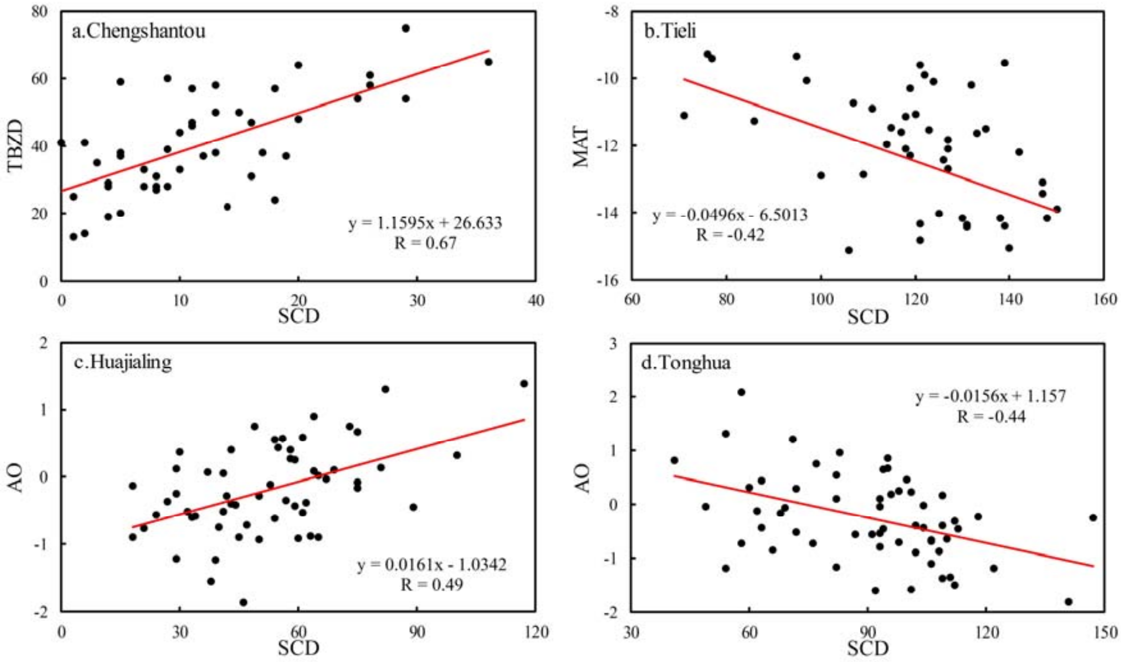

Figure 9